Journal of Magnetic Resonance **148,** 182–199 (2001)
doi:10.1006/jmre.2000.2229, available online at http://www.idealibrary.com on IDEAL®

The Quantum Origins of the Free Induction Decay Signal and Spin Noise

D. I. Hoult and N. S. Ginsberg

Institute for Biodiagnostics, National Research Council, 435 Ellice Avenue, Winnipeg, Manitoba R3B 1Y6, Canada

Received July 28, 2000

Experiments are described that elucidate the quantum mechanical origins of the free induction decay voltage and of spin noise. It is shown that the experimentally measured FID voltage induced in a Hertzian loop receiving coil following a 90° pulse is typically two orders of magnitude too large to be accounted for by the current quantum theory of signal reception—coherent spontaneous emission. An experiment is then presented in which spin noise is easily observed in a circuit with a *Q*-factor of order unity, thereby undermining a popular hypothesis that such noise is due to spontaneous emission and is only observable because of the enhancement in the density of the radiation field in a high *Q*-factor tuned circuit, the NMR probe. Both the free induction decay and the spin noise are shown to be accurately predicted by near-field Faraday induction, which is described in the theory of quantum electrodynamics by an exchange of virtual photons. A heuristic approach to understanding the nature and role of virtual photons in the signal reception process is then given. Thus current popular statements that observation of the magnetic resonance phenomenon relies on the absorption and emission of radio waves are shown to be wrong.

Key Words: **coherent spontaneous emission; radiation damping; spin noise; Faraday induction; virtual photons.**

INTRODUCTION

Signal Reception

By the middle of the 20th century, the quantum theories of matter and its interaction with radiation were well established (*1*). Thus with the discovery of NMR by Bloch and Purcell, a quantum explanation of the voltage present in a receiving coil was sought. However, such an explanation was not readily forthcoming. Bloch had described his observations in terms of Faraday induction while Purcell saw his as absorption and emission of energy, and two initially had great difficulty believing that they were observing the same phenomenon. In particular, describing the origins of the free induction decay caused significant problems, and as the proffered explanation of this phenomenon is still only well known to a handful of NMR physicists, we therefore begin by describing its origins.

In a paper published in 1968, entitled "How does a crossed-coil NMR spectrometer work?" (*2*), Macomber summarizes the dilemma thus: "The fact that the signal persists after the irradiation from the transmitter ceases is . . . proof that neither absorption nor stimulated emission is involved." He goes on to say: "It therefore follows that the signal produced in a crossed-coil NMR spectrometer must be due to spontaneous emission. However, it must be a very strange kind of spontaneous emission: Bloembergen and Pound (*3*) computed the half-life of an NMR excited state that one should expect to be associated with this relaxation mechanism. For a proton in a magnetic field of 10^4 oersteds [1 T], it turns out to be 10^{25} seconds—about 10^8 times the estimated age of the universe. This mechanism would therefore produce a very feeble NMR signal indeed."

[The probability of spontaneous emission I_0 of a photon for a spin-1/2 magnetic dipole in free space is, in SI units,

$$I_0 = \frac{\mu_0 \omega_0^3 \gamma^2 \hbar}{6\pi c^3}, \qquad [1]$$

where μ_0 is the permeability of free space, ω_0 is the Larmor frequency, γ is the magnetogyric ratio, $\hbar$ is Planck's constant divided by 2π, and c is the speed of light. However, there are inconsistencies between various authors in this and other equations. Here, we use Abragam's version (*4*) which yields 3.58×10^{-25} at 1 T.]

Macomber goes on to describe a solution to this problem, realized by Dicke and described in a classic paper published in 1954 (*5*). Dicke had collaborated with Purcell and was well aware of the latter's work and his views that emission of radiation was behind the reception of the NMR signal (*6*); however, his two references to NMR are to Hahn's work on the FID and spin echoes (*7, 8*), probably because here the transmitter is off when the signal is received. Dicke realized that spontaneous emission from a single nucleus in an ensemble or "gas" of *n* spins could cause synchronous emission from other nuclei, provided that the phases of the other nuclei's wavefunctions were sympathetic. This is ideally so immediately following the application of a 90° pulse to an NMR sample in a highly homogeneous B_0 field, and Dicke termed the resulting, greatly enhanced emission "coherent spontaneous emission."

1090-7807/01

He gave the new probability of emission from the *entire* sample as

$$I = \frac{I_0 n^2}{4}\left(\frac{\hbar\omega_0}{2kT}\right)^2, \qquad [2]$$

where k is Boltzmann's constant and T is absolute temperature. This results in increased emission by a factor of the order of 10^{11} for a 1-mL sample.

In the same year, 1954, Bloembergen and Pound (*3*) quickly used Dicke's discovery to explain radiation damping. They considered the magnetic resonance experiment, with its use of a high quality factor (Q), tuned receiving coil to be analogous to a coupled pair of circuits, a device that has since received considerable attention from theorists (*9*). They concluded from classical induction calculations à la Bloch that the characteristic time constant of radiation damping was of the order of a second, a far cry from 10^{25} s, and then asked rhetorically how these two results could be consistent. They answered: "This discrepancy is resolved by considering two factors. One is the coherence which exists between the individual proton spins, the other is the increase in the density of the radiation field in the tuned circuit over that in free space . . . . The magnetic radiation density in the coil of volume V_c of a resonant circuit is increased over the density in free space by a factor . . .:"

$$\eta = \frac{3\pi c^3 Q}{\omega_0^3 V_c}. \qquad [3]$$

(Again, we use Abragam's formulation (*4*).) They go on to describe how, in the presence of coherent spontaneous emission, the damping time constant is now decreased by a factor of n. Then, by multiplying Eqs. [1] and [3] and the number of spins in the system,

$$n = \frac{\mathcal{M}_0 V_m}{\gamma\hbar}\,[\text{sic}], \qquad [4]$$

where $\mathcal{M}_0$ is the equilibrium magnetization and V_m is the sample volume, plus a factor of $\frac{1}{2}$ to allow for the rotation rather than oscillation of the spin system, they arrive at the same formula that was obtained classically and explain the time constant of the order of a second.

Notwithstanding the (self-canceling) mistakes in the article, this was a triumph and convinced most people that NMR signal reception was completely understood. It was due to coherent spontaneous emission in combination with the increase in the density of the radiation field caused by the tuned circuit. In turn, that increase produced radiation damping and thus signal-to-noise ratio (S/N) and radiation damping were felt to be intimately connected. In truth, however, we must remark that Bloembergen and Pound's paper, as beautiful as it is, predicts the order of magnitude of radiation damping. It does not predict the amplitude of the EMF induced in the receiving coil.

Returning to Macomber's paper (*2*), written some 14 years after Dicke's analysis, he ends by saying: "In conclusion, it has been shown that the crossed-coil NMR spectrometer is a unique kind of instrument, operating not by absorption, spontaneous emission or stimulated emission of radiation in the usual fashion. Rather, the RF signal is produced by coherence brightened spontaneous emission, due to the special phase relationship between the magnetic moments of the nuclei." Rosenthal (*10*) had a few quibbles with some of Macomber's statements (*11*), but Dicke had the final say (*12*), tactfully concluding that both Macomber and Rosenthal were correct, and there the matter has rested since. As a result, as communication has filtered down the academic ladder, NMR is almost universally portrayed in the popular scientific literature and in the imaging community as being the absorption and emission of radio waves.

Spin Noise

The issue of the enhancement in the radiation field caused by a high-Q circuit arose once again in the measurement of NMR spin noise by Sleator and co-workers (*13, 14*). Bloch, in his original full paper on nuclear induction (*15*), had remarked that in the absence of an external RF perturbation, there should be induced in a receiving coil a small noise voltage proportional to $n^{1/2}m$, where m is the nuclear magnetic moment. Classically, this can be considered to be caused by the Brownian motion of the rotating frame magnetization. The bulk equilibrium nuclear magnetic moment vector executes a stochastic trajectory about, but very close to, the z axis, mapping out with time a Rayleigh distribution in its projection on the rotating frame $\tilde{x}\tilde{y}$ plane. The correlation time of the transverse component is, of course, T_2, the transverse relaxation time, and the transverse component induces in the receiving coil a voltage at the Larmor frequency of randomly varying amplitude and phase with correlation time T_2. Sleator *et al.* observed spin noise at low temperature (4.2 K) with a sample in a resonant coil coupled to a SQUID detector and associated its detection with spontaneous emission enhanced by the high Q-factor (7320) of their circuit. They obtained a radiated energy that is comparable with the Nyquist noise power generated in a bandwidth of $1/\pi T_2$ Hz. In subsequent papers, Guéron and Leroy (*16*) and, independently, McCoy and Ernst (*17*), showed that it was possible to observe the noise at room temperature. Guéron and Leroy avoided speculation on the quantum origins of the noise while McCoy and Ernst followed Sleator *et al.*'s lead in linking its detection to spontaneous emission.

In the reception both of the free induction decay signal and of spin noise then, a widespread assumption is that spontaneous emission, be it coherent or simple, is responsible for the observed voltage. The emission is then considered enhanced by the Q-factor of the receiving coil. The evidence offered lies in

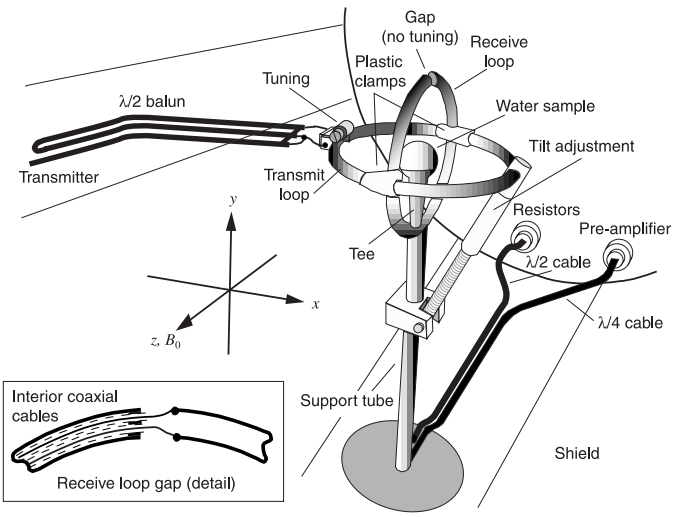

FIG. 1. The crossed-coil probe inside its shield. The interaction between the two Hertzian loops is reduced by a balanced electrical construction and exact orthogonalization with the aid of a plastic screw tilt adjustment. The sample is a ball of doped water. Coaxial cable connections to the *untuned* receiving loop gap are through the inside of the loop and its support.

the absence of any other known mechanism, as described by Macomber, and the comparability of received and emitted energy. However, a series of experiments will now be described that gives evidence that spontaneous emission is not the origin of either the FID or the spin noise voltage. We shall then give heuristic arguments as to why the emission of virtual photons describes the origins of both voltages, thereby avoiding the difficult mathematics of quantum electrodynamics that is outside the scope of this journal. Finally, as a postscript and in view of the controversial nature of the paper, a full description of the rather difficult, radiofrequency experimental details will be given so that others may reproduce the results.

THE FREE INDUCTION DECAY

Results

In deference to Macomber, the cross-coil probe of Fig. 1 was constructed for operation at 63.877 MHz in a 1.5-T imaging magnet. It utilizes two orthogonal Hertzian loops with a ball of doped water for a sample, and strenuous efforts were made to ensure that the two coils were adequately decoupled (<-80 dB) and that radiation damping was minimized. Unusually and significantly, the receiving loop (radius 50 mm) is *untuned* and operates via a $\lambda/4$ line into a low-noise preamplifier followed by an oscilloscope, as indicated in the equivalent circuit of Fig. 2. A $\lambda/2$ line is also attached across the loop gap and, on its end, various loading resistors R_v can be attached. In the figure, R_c represents the loss in the line, L_1 is the receiving coil inductance that is assumed for the time being to have negligible resistance, and R_{in} is the preamplifier input resistance as transformed by the $\lambda/4$ cable. ξ is the FID voltage. The apparatus is described fully in the postscript (Experimental Details) and the extreme care taken to characterize and calibrate the receiving measurement chain is also described there. In not tuning and matching the receiving loop, the underlying design philosophy is to remove the enhancement factor of Eq. [3] provided by the high Q-factor of a tuned receiving coil or "cavity" and then, following a 90° pulse, measure the FID voltage across the coil terminals under various resistive load conditions and compare it with theory. We expect that the measured voltage V_{in} will conform to the dictates of classical network theory; in other words, it will be given by an induced EMF ξ attenuated by the potential divider comprising the coil inductance and the effective resistance R_{eff}:

$$V_{in} = \xi \frac{R_{eff}}{R_{eff} + j\omega_0 L_1}; \quad R_{eff} = \left(\frac{1}{R_c} + \frac{1}{R_v} + \frac{1}{R_{in}}\right)^{-1}, \quad [5]$$

where $j = \sqrt{-1}$.

A plot of measured $|V_{in}|$ versus total resistance R_{eff} across the receiving coil confirms the expectation and is shown in Fig. 3 for various resistance values. A weighted least-squares fit with standard deviations, conforming to Eq. [5], is shown by the dashed lines. The weighting function employed for the fit was the reciprocal of $(d\xi/dR_{eff})^2 + (d\xi/dV_{in})^2$. From the fit, the coil reactance was found to be $63.5 \pm 0.6\ \Omega$, in reasonable agreement with the theoretical value of $67 \pm 2\Omega$ (see Experimental Details), given that a stray capacitance of only 1 pF can reconcile the two values. The amplitude of the EMF from the fit was found to be $\xi_0 = 0.645 \pm 0.003$ mV. The error estimate includes the effects of allowing the loop reactance to vary by $\pm 5\Omega$. However, the systematic uncertainty in the effective gain of the measurement system reduced the accuracy to ± 0.008 mV.

Clearly and unsurprisingly, these seemingly mundane, albeit difficult to obtain, experimental data can be fitted with good accuracy by the electrical model of Eq. [5], viz. an EMF and a potential divider. However, and importantly, if this model which has been accepted for general electrical use for more

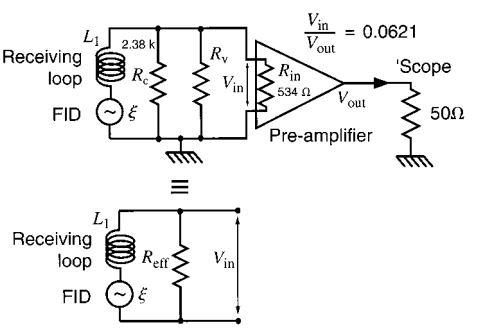

FIG. 2. The equivalent circuit of the preamplifier and the lines shown in Fig. 1 when connected to the receiving loop L_1. The loss in the $\lambda/2$ line is represented by R_c, while its terminating resistance is R_v. The input impedance of the preamplifier as transformed by the $\lambda/4$ line is R_{in}. The effective gain from preamplifier input to oscilloscope screen is 16.1.

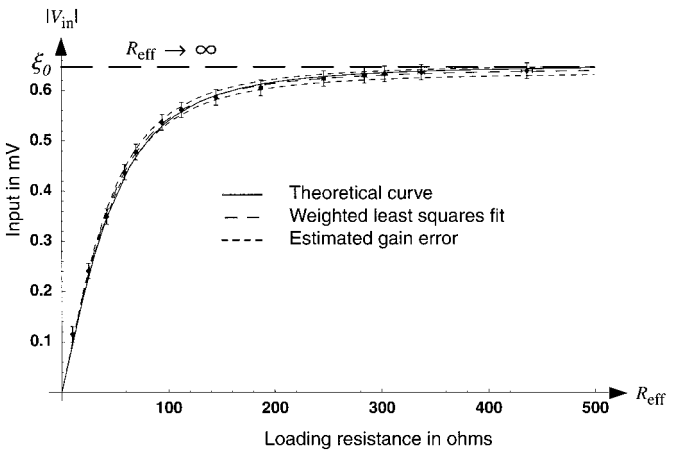

FIG. 3. A plot of measured FID voltage amplitude at the preamplifier input versus total loading resistance across the receiving loop. The error bars concern the estimated accuracies of measurements on the oscilloscope in the presence of noise and of resistances at 64 MHz, and they do not include any systematic error in the estimated gain of the preamplifier. This is shown separately by the dashed lines surrounding the fit to the experimental data. The solid line is the theoretical function predicted by classical electrodynamics and the bulk nuclear magnetic moment. The implication of the measurements is that as $R_{\text{eff}} \to \infty$, a constant EMF of amplitude ξ_0 is present.

than a century is correct, the voltage V_{in} is present even if the connections to the receiving loop are broken ($R_{\text{eff}} \to \infty$ in Eq. [5] and $V_{\text{in}} \to \xi$) and the circuit is open. In this case of course, the Q-factor of the "circuit" is zero, *as is the enhancement factor of Eq. [3].* Thus our task must be to explain the origins of this EMF when there is zero beneficial enhancement of the radiation field by the receiving coil.

Theory

With the main magnetic field $\mathbf{B}_0$ in the z direction, consider the electric field $\mathbf{E}$ generated at a distance $\mathbf{r}$ from a bulk nuclear magnetic moment $\mathbf{M}$ rotating in the xy plane at Larmor frequency ω_0. In SI units, the field is (*18*)

$$\mathbf{E} = \left(\frac{\mu_0}{4\pi r^3}\right)\mathbf{r} \times \left([\dot{\mathbf{M}}] + \frac{r}{c}[\ddot{\mathbf{M}}]\right), \qquad [6]$$

where μ_0 is the permeability of free space and square brackets indicate a retarded function with argument of the form $(t - r/c)$ where c is the speed of light. The superior dots indicate differentiation with respect to time. There are two parts to the equation and it is well known that the first time derivative of $\mathbf{M}$ is responsible for near-field Faraday induction while the second time derivative, or accelerative term, is associated with the radiation field. Let the Hertzian receiving loop have radius r_0 and assume that the NMR sample has negligible spatial extent so that it can be considered at the origin. As the diameter of the sample is considerably smaller than both that of the loop and that of the wavelength of radiation either in the sample or in free space, this assumption should create only a small error which is addressed below. Then the electric field at the loop is in the loop's plane and tangential and is given by

$$E = \left(\frac{\omega_0\mu_0 M}{4\pi r_0^2}\right)\left(1 + j\omega_0\frac{r_0}{c}\right)\exp\left\{j\omega_0\left(t - \frac{r_0}{c}\right)\right\}. \qquad [7]$$

Now the radius r_0 of the loop is such that $\omega_0 r_0/c = 0.045 \ll 1$. We may therefore expand the exponential in Eq. [7] to first order in r_0 with negligible error. Integrating around the loop to find the voltage ξ across its terminals, we then obtain

$$\xi = \xi_0\exp(j\omega_0 t) = \left(\frac{\omega_0\mu_0 M}{2r_0}\right)\left(1 + \frac{\omega_0^2 r_0^2}{c^2}\right)\exp(j\omega_0 t). \qquad [8]$$

The first term in parentheses on the right-hand side of Eq. [8] is the coefficient of the near-field Faraday induction and is in accord with the "Principle of Reciprocity" approach to NMR signal-to-noise ratio calculations (*19*). It is the prototypical expression $\omega_0\hat{B}_1 M$—the angular frequency ω_0 times the field $\hat{B}_1 = \mu_0/2r_0$ at the center of the Hertzian loop due to unit current and times the bulk nuclear magnetic moment M. The radiation term $\omega_0^2 r_0^2/c^2$ modifies the expression but for our experiment it is negligible, comprising only 0.2% of the total.

To compare Eq. [8] with experiment, we must know the strength of the bulk nuclear magnetic moment M. Following a 90° pulse for a sample at equilibrium, it is $M = m\delta n$ where the proton nuclear magnetic moment $m = \gamma\hbar/2$ and δn is the energy level population difference for a spin-1/2 nuclear system of n components at equilibrium at temperature T. γ is the magnetogyric ratio and $\hbar$ is Planck's constant divided by 2π. If k is Boltzmann's constant and $T = 295$ K,

$$\delta n = \frac{n\hbar\omega_0}{2kT} \qquad [9]$$

(*4*), and as the ping-pong ball water sample has a mass of 26.24 g, $M = 1.289 \times 10^{-7}$ Am^2. We assume that the radius r_0 in Eq. [8] is the average radius of the receiving loop, 50.15 mm. (This value may be a little in error as RF current typically flows more on the inner edge of a loop (*19*).) Substituting in Eq. [8] for the described conditions, we obtain a voltage of $\xi_0 = 0.651$ mV, in excellent agreement with the experimental result of 0.645 ± 0.008 mV. We therefore conclude that the FID signal voltage in the open-circuit loop is overwhelmingly the electromotive force associated with near-field Faraday induction. The experiment also confirms the accuracy of the Principle of Reciprocity approach to the calculation of NMR signal reception when the dimensions of the receiving coil are small in comparison to a wavelength. In this regard, it is possible to apply the principle to calculate the loss of signal strength due to B_1 inhomogeneity. It is 0.13%, and the assumption made

above, that the spatial extent of the sample could be neglected, is therefore justified.

We now turn our attention to a quantum description of signal reception. Our aim is to predict the measured EMF in the open-circuit receiving loop for which there is no enhancement of any emission by virtue of a coupled resonator and no enhancing radiation field. We shall need to know the power radiated by the NMR system. Consider the electric field of Eq. [6] $r \rightarrow \infty$. As is well known, only the radiation field with its $1/r$ dependency is of import and is given by the second part of Eq. [6],

$$\mathbf{E} = \left(\frac{\mu_0}{4\pi c r^2}\right)\mathbf{r} \times [\ddot{\mathbf{M}}]. \qquad [10]$$

The field is tangential to the surface of the sphere of radius r and employing the vector identity

$$(\mathbf{a} \times \mathbf{b}) \cdot (\mathbf{c} \times \mathbf{d}) = (\mathbf{a} \cdot \mathbf{c})(\mathbf{b} \cdot \mathbf{d}) - (\mathbf{a} \cdot \mathbf{d})(\mathbf{b} \cdot \mathbf{c}),$$

while remembering that the magnetic moment is in the xy plane, we obtain for the magnitude of the time-averaged Poynting vector P

$$P = \frac{\langle \mathbf{E} \cdot \mathbf{E} \rangle}{Z_0} = \left(\frac{\omega_0^4 \mu_0^2 M^2}{32\pi^2 c^2 r^2 Z_0}\right)(2 - \sin^2\theta), \qquad [11]$$

where θ is the declination of radius vector $\mathbf{r}$ to the z axis, and Z_0 is the characteristic impedance $\mu_0 c$ of free space. Integrating over the surface of the sphere to obtain the total radiated power W_e, we obtain

$$W_e = \frac{\mu_0 \omega_0^4 M^2}{6\pi c^3}. \qquad [12]$$

This value is twice the well-known result for power radiated by an *oscillating* magnetic dipole (*18*), as befits a *rotating* dipole. For our experiment, $W_e = 1.07$ pW.

Turning now to Dicke's analysis of coherent spontaneous emission (*5*), we may multiply Eq. [2] for the emission probability by $\hbar\omega_0$ to find the radiated power. Using Abragam's expression from Eq. [1] for I_0, it may be shown to be exactly Eq. [12]. In other words, the quantum theory of coherent spontaneous emission predicts the classically derived power radiated as radio waves. Thus we have confirmed the accuracy of Dicke's work and, incidentally, confirmed that Abragam's expression for the probability of spontaneous emission is the correct one. However, it is now clear that coherent spontaneous emission cannot be the origin of the FID signal, for the contribution to that signal from the radiative term in Eq. [8] is negligible (0.2%). It is stressed that no mistake has been found in Dicke's *calculations;* his error was in agreeing with Macomber in assuming that they were applicable to the NMR free induction decay. Given that, to this day, spontaneous and stimulated emission are still the cornerstones by which the production of photons are understood, the assumption is not surprising. However, the unavoidable conclusion must be that photons produced by spontaneous emission, albeit coherent, cannot be the source of the NMR free induction decay.

SPIN NOISE

Theory

We now turn our attention to the origins of spin noise. Sleator *et al.* (*14*) were careful not to claim that spontaneous emission was the *cause* of spin noise, but in the presumed absence of any other mechanism, a common interpretation of their paper is that such emission, coupled with radiation field amplification by a high Q-factor, *is* responsibe. However, if it is possible to observe spin noise in the absence of a high Q-factor, this interpreation must be in doubt. In particular, if classical electromagnetic theory indicates that a random voltage due to spin noise is present in an open-circuit coil, so that the amplification factor of Eq. [3] is zero, then unenhanced spontaneous emission, with its incredibly low probability, must be dismissed out of hand. Thus our aim in this section is to see whether it is possible to devise an experiment where spin noise can be observed in the same manner that we observed a FID—with a high input impedance preamplifier connected directly to a receiving coil and with the implication that the noise voltage is still present in the coil even if it is open-circuit.

A standard way of approaching the calculation of any noise phenomenon is the Fluctuation Dissipation theorem, which is an application of the Principle of Reciprocity. We expand here on the approach used by previous workers (*13, 14, 16, 17*) but quote Helstrom's book on stochastic processes (*20*): "Whenever a mechanism exists by which coherent energy is converted to heat, *that same mechanism* manifests a randomly fluctuating force when the system is in thermal equilibrium, and the spectral density of that force is proportional to the same constant as determines the rate of conversion of work into heat" (our emphasis). In other words, if application of a voltage to a coil causes a current to flow, that produces a *near* magnetic B_1 field, which causes the NMR system to absorb energy, which is subsequently turned to heat; then a random EMF must be induced in the coil by the same mechanism—by a near magnetic field, i.e., Faraday induction. Thus the Fluctuation Dissipation theorem, which is proved in detail by Helstrom, gives theoretical cause for belief that spin noise is a near-field phenomenon, for the B_1 field used in a typical CW saturation experiment is certainly near-field. Sleator *et al.* (*14*) and McCoy and Ernst (*17*) invoked the mathematics of the theory in the guise of Nyquist's formula, as we are about to do, but did

not employ the genetic details of the theory as so eloquently expressed by Helstrom.

To apply the theorem, we consider a continuous wave experiment in which a coil produces an alternating, near magnetic field of amplitude $\hat{B}_1$ in the x direction when current of unit amplitude at frequency ω is passed. Let a current of amplitude i_0 at that frequency be applied continuously and let there be in the coil a sample of bulk equilibrium nuclear magnetic moment M_0. Then the field in the rotating frame is $i_0\hat{B}_1/2$ and if we define the field to be along the $\tilde{y}$ axis, the equilibrium solution of the Bloch equations for the magnetic moment in the rotating $\tilde{x}\tilde{y}$ plane is (*4*)

$$\tilde{M}_x = \frac{0.5\gamma i_0 \hat{B}_1 T_2}{1 + (\Delta\omega T_2)^2 + 0.25(\gamma i_0 \hat{B}_1)^2 T_1 T_2} M_0 \qquad [13]$$

$$\tilde{M}_y = \frac{-0.5\Delta\omega\gamma i_0 \hat{B}_1 T_2^2}{1 + (\Delta\omega T_2)^2 + 0.25(\gamma i_0 \hat{B}_1)^2 T_1 T_2} M_0, \qquad [14]$$

where $\Delta\omega = \omega - \omega_0$, T_1 is the longitudinal relaxation time, and we have assumed right-hand rotation. The amplitude of the Faraday voltage induced in the coil by the precessing nuclear magnetic moment, neglecting the tiny radiative contribution, is, from Eq. [8],

$$\xi_0 = \omega\hat{B}_1(\tilde{M}_x + j\tilde{M}_y), \qquad [15]$$

and by Ohm's law, the effective impedance that the NMR sample creates in series with the coil's impedance is

$$Z_n = \frac{\xi_0}{i_0} = \frac{0.5\omega\gamma\hat{B}_1^2 T_2(1 - j\Delta\omega T_2)}{1 + (\Delta\omega T_2)^2 + 0.25(\gamma i_0 \hat{B}_1)^2 T_1 T_2} M_0. \qquad [16]$$

Hence,

$$\underset{i_0\to 0}{\text{Limit}}[Z_n] \equiv R_n + jX_n = \frac{0.5\omega\gamma\hat{B}_1^2 T_2}{1 + j\Delta\omega T_2} M_0 \qquad [17]$$

and the effective resistance R_n is the absorption part (appropriately) of a Lorentzian. As the energy stored by a magnetic moment $\mathbf{M}$ in a field $\mathbf{B}_0$ is $-\mathbf{B}_0 \cdot \mathbf{M}$, an alternative way of deriving the real part of Eq. [17] is by considering the power absorption W

$$W = -B_0 \frac{dM_z}{dt} = -B_0 \frac{(M_z - M_0)}{T_1}, \qquad [18]$$

where we have used one of the Bloch equations and the continuous wave equilibrium expression for M_z (*4*) must be applied.

Now the spectral density function of the received noise EMF is

$$S(\omega) = 4kTR_n, \qquad [19]$$

in other words, Nyquist's formula (*20*). Using Eq. [17] for the NMR resistance R_n and Eq. [9] to find the equilibrium bulk nuclear magnetic moment M_0, we have

$$S(\omega) = (\omega_0\hat{B}_1 m)^2 n \frac{2T_2}{1 + (\Delta\omega T_2)^2}, \qquad [20]$$

where we have set $\omega = \omega_0$ with negligible loss of accuracy and remembered that $m = \gamma\hbar/2$. Integrating over frequency difference $\Delta\omega$, we may find the root mean square noise in the time domain. It is (*20*)

$$N_{\text{NMR}} = \left[\int_0^\infty S(\omega)\frac{d\omega}{2\pi}\right]^{1/2} = \omega_0\hat{B}_1 m\sqrt{n} \qquad [21]$$

and Bloch's insight (*15*) is validated. However, once again we have the $\omega_0\hat{B}_1$ multiplier that is characteristic of Faraday induction and the Principle of Reciprocity. By the Central Limit theorem (*20*), the equation can be construed as representing the induced RMS Gaussian noise from n units ($n \gg 1$) of a quantity having a variance of m^2, which implies discrete values of $\pm m$ rather than a distribution. In other words, the nuclear spin is quantized in the rotating frame transverse plane. Note that with this approach to the calculation of the noise, the quantization in the transverse plane is forced upon us as a direct consequence of the formulation of M_0, which is from quantum statistics. Moreover, it would appear that we can calculate the quantized voltage $\omega_0\hat{B}_1 m$ from a single nucleus and simply multiply by $\sqrt{n}$ to obtain the full spin noise voltage! A justification for this heretical viewpoint will be given later.

Having obtained simple formulae for the noise, we must now determine whether the latter is sufficiently large to be seen without Q-enhancement. Field effect transistors operating at 64 MHz can have superb noise figures when working from a source of resistance $\sim$1 kΩ, and by scrupulous attention to detail, noise figures of under 0.5 dB can even be obtained with source resistances as low as 50 Ω. In other words, it is possible for the preamplifier to add less than 6% extra noise to that generated by a 50-Ω resistor at room temperature. Thus our aim must be to generate a receiving coil and sample that give on resonance an NMR resistance R_n that is at least 50 Ω, so that we can be sure that any spin noise spectrum we obtain is not the result of stimulation of the NMR system by current noise from the preamplifier. From Eq. [17] it follows that we must maximize the on-resonance resistance:

$$R_{n0} = 0.5\omega_0\gamma\hat{B}_1^2 T_2 \mathcal{M}_0 V_s, \qquad [22]$$

where V_s is the sample volume and $\mathcal{M}_0$ is the equilibrium

magnetization. A solenoid is generally considered to be the most efficient receiving coil. The B_1 field at its center due to unit current is given by (*21*)

$$\hat{B}_1 = \frac{\mu_0 N}{2} (a^2 + g^2)^{-1/2}, \qquad [23]$$

where N is the number of turns, a is its radius, and g is its half-length. Now the length of wire on a solenoid for efficient operation well below self-resonance should not exceed roughly $\lambda/20$ (*22*), where λ is wavelength. Thus we set $N = c/20a\omega_0$. Remembering that the magnetization $\mathcal{M}_0$ is proportional to frequency, it follows that the resistance R_n is now roughly independent of frequency. Hence we should work at a low B_0 field strength to maximize absolute field homogeneity and, with it, the maximum value of T_2 that can gainfully be used. (Note that Eq. [22] is independent of T_1.) Setting the effective volume of the sample to approximately $2\pi a^2 g$, we may see from Eqs. [22] and [23] that the NMR resistance is proportional to $g/(a^2 + g^2)$. Thus the solenoid should be equal in length to its diameter and as *small* as possible. Evaluation of Eq. [22] at 64 MHz, with 20 turns of wire covering 5 mm on a 5-mm diameter with water as a sample, shows that a resistance of the order of 50 Ω can be reached if a linewidth of under 2 Hz can be attained. (The calculation is only accurate to, say, ±20%, as we have accommodated B_1 field inhomogeneity by making the effective sample volume that of the coil. If necessary, a computer simulation can give a more exact value.)

The inductance of such a solenoid is given by the Nagaoka formula (*23*) as 1.6 μH and, thus, with an anticipated Q-factor of the order of 100 (*22*), its impedance at 64 MHz may be predicted as roughly $6 + j550$ Ω. Thus the resistance r_c of the coil is not an obstacle to accurate spin noise measurement, but the reactance is, even though it generates of itself no noise, for the following reason. The standard noise equivalent circuit of an RF preamplifier (*24*) (considered further under Experimental Details and shown in Fig. 10b) contains both a noise voltage source V_n and a constant current noise source I_n which may be partially correlated. For a preamplifier optimized for 50-Ω usage with a noise figure of 0.5 dB, a typical value for the current source is easily shown to be 3 pA/√Hz (voltage and current correlated), which would therefore generate about 1.7 nV/√Hz across $j550$ Ω. Unfortunately, the noise from a 50-Ω resistor is only about 1 nV/√Hz, and this would therefore be masked by the voltage created by the current noise. It follows that unless we can obtain a preamplifier with an impossibly low noise figure, we have no option but to cancel the inductive reactance with a *series* capacitance. We should then be able to connect the combination to the preamplifier and detect the spin noise directly, secure in the knowledge that the current noise is contributing only a small fraction of the observed noise peak at the Larmor frequency. However, in being forced to use a capacitor between the coil and the preamplifier, remembering that the input resistance of the preamplifier with its $\lambda/4$ cable is of the order of 500 Ω, we will have made a very low-Q (~1) tuned circuit, which we would really have preferred to have avoided.

Results

The receiving coil described above was built with nominally zero-susceptibility wire (albeit with a length of 6 mm, not 5 mm, to minimize B_0 field inhomogeneity caused by residual susceptibility) as shown in Fig. 4, on a 5-mm NMR tube and used with a homemade shim set. A linewidth of 1.8 Hz was obtained, with the sample unspun. Full details are given under Experimental Details. A CW experiment was then performed to determine the coil and NMR resistances r_c and R_n. Essentially, a known current was passed through the coil and the voltage across the latter was measured. Well off resonance, the resistance r_c was found to be 8 Ω, considerably less than the desired NMR spin noise resistance of 50 Ω. On resonance, R_n was found to be 65 ± 4 Ω, in good agreement with the theory above, considering that the effects of B_1 inhomogeneity have only been crudely accommodated and that T_2^* rather than T_2 described the transverse relaxation. The same preamplifier as before was used and the noise figure, with cables and transmit/receive switch attached, was found to be 0.7 dB. (The switch was used for setup purposes only and the transmitter was disconnected during noise measurements.) Thus 92% of the noise measured from a 50-Ω resistor at room temperature was still from the resistor itself and we would expect a similar proportion to hold for the NMR spin noise too. (The remaining 8% is from voltage noise in the preamplifier and current noise "driving" the resistor or NMR system.)

The coil and its tuning capacitor were temporarily replaced by a set of resistors (10–100 Ω) and their noise spectral densities, over a bandwidth of 1 kHz with a resolution of 0.488 Hz, were now measured. The spectral density functions, an example of which is shown in Fig. 5a, provided a calibration (noise vs resistance) of the spectrometer. The increase toward the Nyquist frequencies is caused by the poor spectrometer filters, which permitted aliasing. The spectral density function of the spin noise was also measured and is shown in Figs. 5b and 6. Proof that there was no coherent component to the spectra is given under Experimental Details. Averaging the spectral baseline in Fig. 6, the background resistance due to the coil is 9 Ω, as may be seen from the plot's calibration lines, in good agreement with a network analyzer measurement of 8 Ω and the value from the CW experiment above. The peak resistance, the sum of the coil and NMR resistances, is 71 ± 3 Ω. Thus the NMR resistance of 62 ± 3 Ω obtained from a spin noise measurement is in good agreement with both theory and the CW measurement.

We have viewed spin noise in the absence of a high Q-factor circuit and in good agreement with a theory derived from near-field considerations. The implication of the experiment is

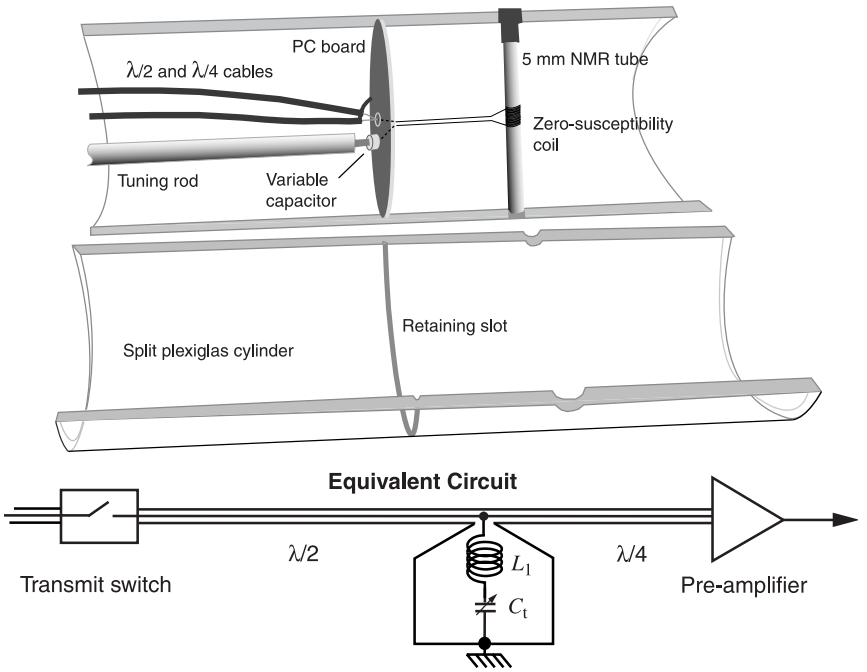

FIG. 4. The spin noise probe and its equivalent circuit. Note the absence of parallel tuning, the grounded variable capacitor being in series with the coil. The tube of water and a circular printed circuit board are mounted in a "Plexiglas" cylinder. The board is distant from the coil to reduce B_0 field perturbations at the sample. Once the two halves of the cylinder have been mated, the whole is mounted in a shielded shim set. A linewidth of 1.8 Hz was obtained.

that the noise voltage is an EMF that is present even if the preamplifier is detached and the receiving coil is open-circuit. It is then inconceivable that spontaneous emission could cause such a voltage. We considered repeating the measurement of the spin noise spectrum with various loading resistances across the receiving coil in order to emulate the philosophy used in determining that the FID signal was a near-field electromotive force. However, given that we had essentially already placed an arbitrary resistance across the coil (the preamplifier plus cables), we felt that this heavy labor would add little new evidence to that already provided by the agreement between theory and experiment.

RADIATION DAMPING

It is tempting now to turn directly to the proposed origins of the FID and spin noise—virtual photons. However, it is also important to clarify why Bloembergen and Pound were able to predict "radiation" damping so well and to examine the origins of a supposed link between the latter and signal-to-noise ratio. Considering a pulse experiment on an *average* spectrometer (not our special instrument) and invoking the electrical engineering topic of network theory, an electrical network of some sort typically links the receiving coil to the preamplifier's active device, say a FET. Looking *from the preamplifier to the coil*, the network's purpose is to transform, with as little extra resistance as possible, the source impedance (the coil reactance and its resistance) to that value which allows the preamplifier to deliver its optimum noise figure (*24*). In this process the EMF induced in the coil by the NMR sample is also transformed, in accord with the conservation of energy. (A straightforward analysis of the standard noise-equivalent circuit given in Fig. 10b will confirm that there is an optimal source resistance for best S/N.) However, at any one specific frequency, no matter how complicated the noise-matching network may be (tuning and matching capacitors, lines, etc.), by Thévenin's theorem (*25*) a terminated network may be considered a single impedance. Thus the schematic of Fig. 7 summarizes that network *when looking from the probe to the preamplifier*. Here, we have assumed that the input impedance of the preamplifier is resistive. Note that the forward and reverse transformations of a network are not necessarily symmetrical. The forward impedance Z_{Th} may well, to high accuracy, be capacitive with negligible resistance such that the inductance of the receiving coil is cancelled. Two limiting cases are then of import: when $R_{\mathrm{Th}} \gg r_{\mathrm{c}}$ and vice versa. In practice, the coil inductance may not be fully cancelled and an intermediate value of R_{Th} is usually obtained, although it is important to realize that the value of R_{Th} is under the control of the circuit designer to a considerable degree.

$R_{Th} \gg r_c$, Reactance Annulled

Clearly, when an EMF is induced in an open-circuit coil ($R_{\mathrm{Th}} \rightarrow \infty$), no power is dissipated. As soon as the preamplifier and any intervening network are connected to the receiving coil

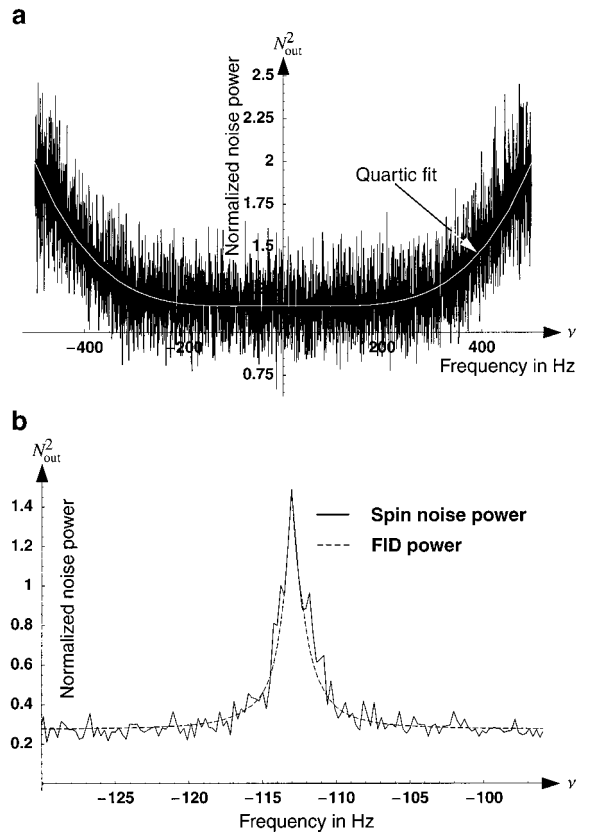

FIG. 5. In (a), the 1-kHz bandwidth, normalized, noise power spectrum from a 50-Ω resistor at room temperature, as collected by the spectrometer, is shown. (Ordinate unity represents the theoretical noise from 50 Ω at 293 K.) The spectrum is part of a calibration of the experiment and the rise at the extremities is due to noise aliasing. Spectra from different resistances will have, of course, greater or lesser noise powers. (b) Shows the spin noise power spectrum from the water sample (64 data sets of 2048 points, 1 ms per point) and the power spectrum from the FID. The two are similar.

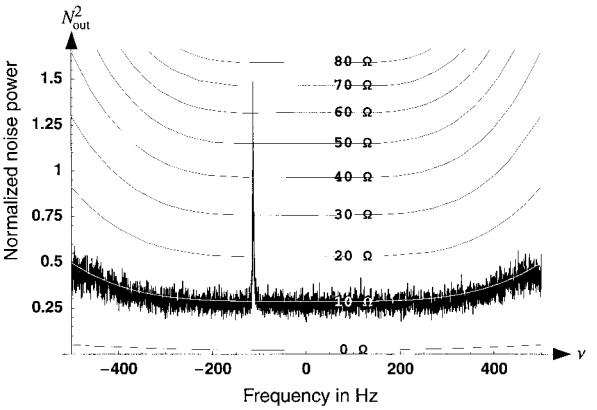

FIG. 6. The calibrated spin noise spectrum showing clearly an on-resonance resistance of about 71 Ω. Calibration was performed with quartic plots of the form of those in Fig. 5a. The coil resistance of approximately 9 Ω and the residual noise from the preamplifier causes the spectrum to be offset from the baseline. Note the small height of the 0-Ω calibration curve, a measure of the preamplifier's very small voltage noise contribution.

though, the power dissipated immediately following a 90° pulse is

$$W_d = \frac{\xi_0^2}{2R_{Th}} = \frac{(\omega_0 \hat{B}_1 M_0)^2}{2R_{Th}}; \quad R_{Th} \gg r_c, \qquad [24]$$

where the factor of 2 in the denominator is present because the *amplitude* of the EMF has been employed. This power is supplied, of course, by the NMR system—we have "radiation" damping—and some, perhaps most, of the power goes to modulating the current in the FET which in turn provides amplification. As the system's stored energy is $(M_0 - M_z)B_0$, M_z increases as energy is extracted and the transverse component of magnetization diminishes. However, in the average NMR experiment when $R_{Th} \gg r_c$, the received noise is a function of the coil resistance r_c, not of R_{Th} or R_n (*19*). It immediately follows that there is, in this instance, no relationship between S/N and "radiation" damping, for coil resistance r_c is not involved in Eq. [24].

$R_{Th} \ll r_c$, *Reactance Annulled*

When we choose, either deliberately or by bad engineering, to apply a negligible dissipative load to the circuit ($R_{Th} \to 0$), maximal power is deposited overwhelmingly in the coil's resistance r_c and we may obtain the power's value simply by substituting r_c for R_{Th} in Eq. [24]. However, the circuit noise voltage N_c, by Nyquist's formula (*20*), is $4kTr_c$ per root unit

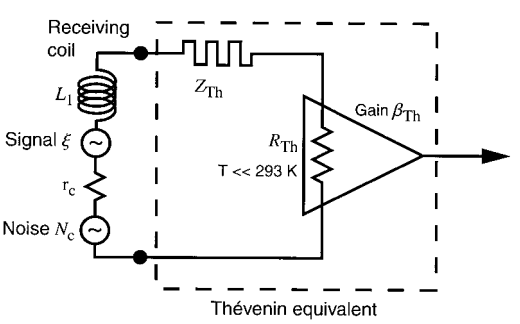

FIG. 7. The forward Thévenin equivalent circuit (i.e., looking toward the preamplifier) of the noise-matching network connecting the receiving coil to the preamplifier in an average spectrometer. The input of the preamplifier is assumed to be resistive. *All* quantities within the dashed line are transformation- (and therefore frequency-) dependent. At the Larmor frequency, the impedance Z_{Th} may well be almost purely capacitive such that it cancels the inductive reactance of the receiving coil. The probe noise is assumed to arise from the resistance r_c of the receiving coil. Note the effective temperature of the preamplifier. Looking from the preamplifier to the probe, a different Thévenin equivalent is needed.

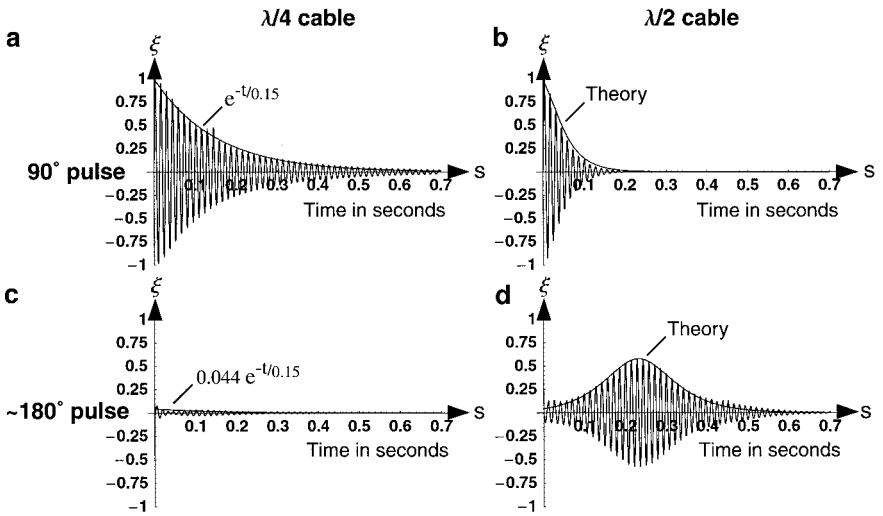

FIG. 8. So-called "radiation" damping. Using the spin noise experimental setup of Fig. 4, the FID following a 90° pulse is shown in (a). It can be roughly fitted with an exponential decay of time constant 150 ms, although there is a "tail" to the FID that results in a linewidth that is slightly less than 2 Hz. In (b), an extra λ/4 cable is inserted between the coil and the preamplifier so that the latter's input resistance becomes roughly 5 Ω rather than 550 Ω. Extreme damping is immediately visible. In (c) and (d) the experiment is repeated with a nominally 180° pulse. The fits to the curves were obtained with a numerical solution of the Bloch equations. All curves were normalized to an amplitude of unity to remove the effects on gain of impedance transformations with change of cable length.

bandwidth. Thus, substituting this in Eq. [24] we have that the power per unit bandwidth is

$$W_d = \frac{\xi_0^2}{2r_c} = 2kT\left(\frac{\xi}{N_c}\right)^2; \quad R_{Th} \ll r_c, \qquad [25]$$

and we have the origin of the supposed connection between "radiation" damping and S/N ratio. (Note that ξ and N_c are both attenuated as $R_{Th}/(R_{Th} + r_c)$ upon entering the preamplifier.) However, the decision to construct the network between the receiver and the preamplifier such that $R_{Th} \ll r_c$ lies entirely in the hands of the designer. A graphic illustration of this fact may be had with our noise coil (Fig. 4), whose sensitivity is sufficiently large to reveal "radiation" damping. Figure 8a shows the FID following the 90° pulse that was used for initial shimming purposes. It has roughly an exponential decay with time constant 150 ms. However, Fig. 8b shows the effects of merely adding an extra λ/4 cable between the probe and the preamplifier. There is large damping caused by the fact that there is now a low resistance instead of a high resistance across the receiver coil; by Ohm's law, much more power is extracted from the NMR system. The extent of the damping is easily calculated, as is well known, and a fit from the Bloch equations is given, as are results following the application of a nominally 180° pulse.

We cannot stress too strongly that the role of a tuned circuit in a modern NMR probe has nothing to do with signal and radiation field enhancement. The creation of a tuned circuit is a by-product of the need to transform with a network the source impedance of the NMR signal to a value, say 1 kΩ resistive (perhaps via a 50-Ω intermediary), that allows a semi-conductor to contribute negligible additional noise to the experiment. The crudest way of accomplishing this goal is by the addition of two capacitors to the coil, one in series and one in parallel, and this act unfortunately creates a high-Q, parallel tuned circuit that has been seized upon as being a necessary part of the NMR protocol. We have shown that it is not necessary, merely desirable. Nowadays, more sophisticated impedance transformation techniques can be used, and the essence of good probe and receiver design is to maximize signal-to-noise ratio by optimizing source impedance while minimizing power dissipation and damping, i.e., while maximizing R_{Th}. Figure 9, which illustrates part of the transmission circuitry described under Experimental Details, shows in principle one of several ways in which this goal can be accomplished. We substitute the high-input impedance preamplifier for the switch box and utilize the transmitting coil as a receiver. The preamplifier then "sees" the desired source impedance, but the receiver coil is in series with a moderately high resistance (created by preamplifier input impedance in parallel with the line and capacitor C_m which are parallel-resonant), which curbs current flow and hence greatly reduces damping. In the present context, this topic is explored in more detail in Ref. (*26*), while an excellent discussion of semi-conductor noise and low-noise circuit techniques may be found in the book by Motchenbacher and Connelly (*24*). It should be noted that the use of Q-damping by the preamplifier, without loss of S/N, has been in widespread use in NMR imaging for several years (*27, 28*). In fields such as ESR, the technique is often known as "overcoupling." To summarize, "radiation" damping is almost entirely under our control by our choice of resistance R_{Th}.

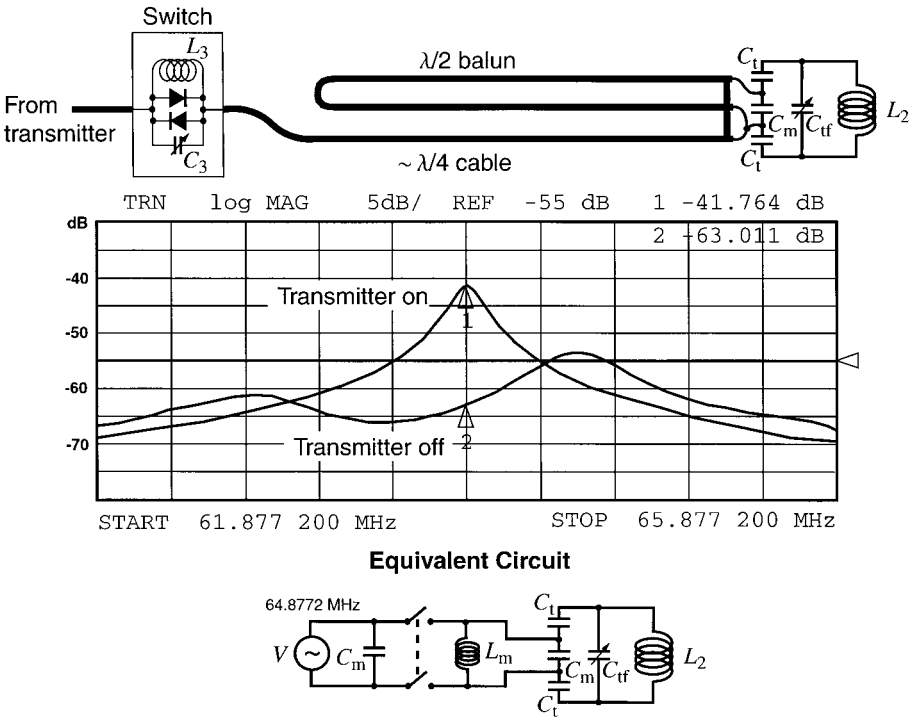

FIG. 9. Electrical details of the transmitter loop circuitry. The network analyzer response versus frequency of the circuit is plotted at low power with the crossed-diode switch in place (marker 2) and with the switch replaced by 50 Ω (marker 1). The reduction of current flow at the Larmor frequency caused by the switch, and the lines and the capacitors which create a blocking circuit, is 21.2 dB. This translates to an effective "*Q*-spoiling" (and hence decrease in coupling and damping) of 27.2 dB when compared to the unloaded loop, $Q = 750$. The lower part of the figure shows the equivalent circuit of the switch and transmitter probe.

The Enhancement Factor

What then of the enhancement of the radiation field? As a separate matter, the energy stored in an inductor carrying a current i is

$$E = \frac{1}{2} Li^2 = \frac{1}{2} \int \mathbf{B} \cdot \mathbf{H} dV. \qquad [26]$$

Considering a solenoid, the receiving coil used exclusively in early NMR experiments, we may make the crude approximation that roughly half the energy is stored in the volume of the coil, and so $L \approx 2\hat{B}_1^2 V_c/\mu_0$. Hence the Q-factor $\omega_0 L/(R_{Th} + r_c)$ of the *circuit* comprising the solenoid with its series capacitance and resistance $R_{Th} + r_c$ (Fig. 7) is approximately known and, substituting in Eq. [24], we obtain for the initial dissipation of energy during a FID caused by Faraday induction

$$W_d \approx \frac{\mu_0 Q \omega_0 M_0^2}{4V_c}. \qquad [27]$$

For a (impossible-to-make) solenoid quadrature coil, twice this power would be dissipated. If we now take the ratio of this quadrature power to that emitted as coherent spontaneous emission W_e, Eq. [12], we get

$$\eta = \frac{2W_d}{W_e} \approx \frac{3\pi c^3 Q}{\omega_0^3 V_c}. \qquad [28]$$

This is precisely Eq. [3], the enhancement factor for the magnetic radiation density, and we now see this factor in its true colors—it is simply an approximate ratio of the power that we *choose* to dissipate, by putting a resistance R_{Th} across a receiving coil, to that emitted by coherent spontaneous emission. (Note that it is only reasonably valid for a solenoid and would be considerably in error for a Hertzian loop. The so-called "filling factor" would have to be included to restore its accuracy.) However, the amplitude of the EMF is quite independent of the value of R_{Th} and hence η, and to say that it is induced in the coil as a consequence of emission and the magnetic field enhancement is to confuse correlation and cause. The near-field EMF is *correlated* with the far-field emission, as is shown quite clearly in Eqs. [6] through [8], but the *cause* of the EMF is Faraday induction associated with a rotating magnetic moment. Further, the correlation becomes weaker and weaker the lower the frequency, thanks to the different frequency dependencies of emission and induction.

It now should not be surprising that Bloembergen and Pound were able to calculate the order of magnitude of damping correctly. By using the enhancement factor of Eqs. [3] and [28], they were simply finding in a very roundabout manner the power dissipated by the induced EMF. What then of the term "radiation damping?" It is reasonably well known that this is a total misnomer, and "induction damping" would be a far more accurate term as, for all practical situations, the damping is caused overwhelmingly by the energy dissipated in resistance $R_{\mathrm{Th}} + r_{\mathrm{c}}$; in turn, that dissipation is a consequence of the induced EMF, not of radiation, the latter inducing a voltage that is usually negligible.

Spin Noise

Turning to the spin noise experiment, we can also calculate the ratio of the noise power W_{n} that the NMR system deposits in a resistor R_{Th} across the receiving coil to that emitted by spontaneous emission W_{s}. (It is helpful to imagine that the resistor has a temperature of 0 K and has a value very much greater than the spin resistance.) From Eq. [21], remembering that the equation gives an RMS voltage, it is

$$W_{\mathrm{n}} = \omega_0^2 \hat{B}_1^2 m^2 n / R_{\mathrm{Th}}. \qquad [29]$$

We employ again the solenoidal-coil approximation used above for $\hat{B}_1^2/R_{\mathrm{Th}}$ and fictitious quadrature receiving coils. Then from Eq. [1], remembering that only approximately half the spins are in the upper energy level,

$$\eta = \frac{2W_{\mathrm{n}}}{W_{\mathrm{s}}} = \frac{3\pi c^3 Q}{\omega_0^3 V_{\mathrm{c}}}, \qquad [30]$$

and we have once more the enhancement factor for the magnetic radiation density. However, again to say that spontaneous emission is the origin of the noise is to confuse correlation and cause. From Eq. [21], it is clear that Faraday induction is the source of the noise.

DISCUSSION

The overriding issues that need explanation are the quantum origins of Faraday induction and the transfer of energy from the NMR system to resistance R_{Th}. Insight lies in the domain of quantum electrodynamics (QED) and electromagnetic interactions between charged particles have been pondered extensively by Feynman and others (*29–34*), although usually in the context of high-energy nuclear physics. We now therefore briefly tread well outside the NMR discipline and extend the ideas of QED to the very-low-energy situations encountered at radio- and lower frequencies, albeit heuristically and with models, as the mathematics of quantum electrodynamics is specialized, difficult, and well outside the scope of this journal. It is stressed that, in the broader context of theoretical physics, the concept of virtual photons that we are about to explore is well known and reluctantly accepted as being an explanation for near-field phenomena. The reluctance stems from the awkwardness of the model and the impracticality of the associated mathematics.

Consider first a stationary conduction electron in our receiving loop. In some sense the electron is free to move, for if the loop is terminated with a resistance, the electron can accelerate under the influence of an electric field created by a changing magnetic field through the loop. When many such electrons start to move, we say that a current flows. The electrons will, though, eventually deliver up by collision (phonon interaction) their new-found energy as heat, a phenomenon we term "resistance." (The magnetic field is created, of course, by the rotating nuclear magnetic moment.) Now photons are considered to be the carriers of the electromagnetic interaction. Upon being absorbed, their momentum and energy are transferred to the absorber and a force (rate of change of momentum) is created. However, from elementary considerations of conservation of energy and momentum, it is clear that a photon with momentum p and energy $U = \hbar\omega_0 = pc$ cannot be absorbed by our stationary electron. (At radiofrequencies ~100 MHz, the energy in the photon would have to be of $\sim 10^{-13}$ U.) Thus, how can the electron be accelerated? Second, consider the situation when the loop is open-circuit. The electrons now do not accelerate even classically—no current starts to flow—for the induced EMF is countered by an equal and opposite electric field from charge separation. Charge has essentially previously "piled up" at the loop gap under the action of the EMF and generates a counter conservative electric field. We may now consider that the electron is receiving, on average, photons of equal energy and scalar momentum approaching from opposite sides and hence remains stationary (we assume the photon momentum is in the direction of travel), but for this picture to hold, photon energy U would have to be zero!

How, then, can an electric field be communicated by photons? The answer lies in the Uncertainty Principle: for a time Δt determined by the relation $\Delta U \Delta t \sim h$, and therefore over a limited distance $c\Delta t$, the photon energy may be in error by an amount ΔU and, in particular, U may be zero. Thus, both cases described above may be accommodated for short periods of time by invoking photons with the "wrong" energy—virtual photons (*30*). It is of interest to note that the Uncertainty Principle predicts that a zero-energy virtual photon ($\Delta U = \hbar\omega_0$) can exist only for such a time that it exerts influence over a distance of the order of a wavelength. This is, of course, a defining distance for electromagnetic fields—at greater distances, far fields (real photons) dominate, closer to the source, near fields (virtual photons) predominate, in accord with accepted field theory and the two different dependencies upon distance in Eq. [6].

Going even further away from NMR, the case for virtual photons is strengthened when we consider the requirement of

Lorentz invariance for the electric field from a charged particle moving at relativistic speeds. Consider a charge e_1 at the origin of a frame moving with velocity v in the laboratory z direction. It is well known (*35, 36*) that the spatial variation in the laboratory frame of its electric field, relative to the instantaneous *present position* of the charge at point Q, is given by

$$\mathbf{E} = \frac{e_1 \mathbf{r}}{4\pi\epsilon_0 r^3} G(\theta), \qquad [31]$$

where ϵ_0 is the permittivity of free space, $\mathbf{r}$ is the vector distance from point Q in the laboratory frame to a point P of interest, and θ is the declination of the latter relative to the z direction at Q. Here, the distribution function $G(\theta)$ is given by

$$G(\theta) = \left(1 - \frac{v^2}{c^2}\right)\left(1 - \frac{v^2}{c^2}\sin^2\theta\right)^{-3/2} \qquad [32]$$

and at high speeds, note that this function is concentrated in the xy plane perpendicular to the direction of motion. Now consider the charge, stationary in its own frame of reference denoted henceforth by primes. Assume that in that frame it emits photons isotropically and that their impact on any other charges constitutes the central electrostatic force. In particular, we shall be interested in photons emitted at an angle θ' to the z' direction. However, in going from the charge's frame to the laboratory frame, the relativistic transformation equations of the photons' energy-momentum four-vector are (*37*)

$$\begin{aligned} U' &= -pc\cos\theta\sinh\zeta + U\cosh\zeta \\ p'\cos\theta' &= p\cos\theta\cosh\zeta - U\sinh\zeta/c \\ p'\sin\theta' &= p\sin\theta, \end{aligned} \qquad [33]$$

where $\tanh\zeta = v/c$. Now, in general, these equations are totally inconsistent with Eq. [32]. For example, if $U = pc$, as befits a real photon, the emission of such photons can be shown to be concentrated *about* the z axis as $v \to c$ (*37*), not *perpendicular* to it. However, if we take the ratio of the third to second equations [33] with $U = 0$, i.e., for virtual photons with no energy, we obtain

$$\tan\theta = \tan\theta'\cosh\zeta \qquad [34]$$

and at high speeds as $v \to c$, $\theta \to 90°$ perpendicular to the direction of motion. Finding from Eq. [34] the expression for $\cos\theta'$ and differentiating w.r.t. θ', it is then not surprising that

$$\sin\theta' d\theta' = G(\theta)\sin\theta d\theta. \qquad [35]$$

In other words, the distribution function of the photons is just Eq. [32] if they carry no energy and so only zero-energy virtual photons can describe an electrostatic field while fulfilling the requirement of Lorentz invariance. Note that while U' is not zero, the total emitted energy in the moving frame *is* zero—under the auspices of the Uncertainty Principle, negative energies are permitted for a short time—a concept that Dirac wrestled with while trying to predict spin.

A full quantum electrodynamic calculation is needed to *prove* that virtual photons with zero energy carry the electrostatic field, but the above simple analysis gives pleasing heuristic evidence. (An alternative and more elegant derivation may be found from group theory and Noether's theorem (*38*).) How does the above relativistic analysis relate to NMR? Once the Lorentz-invariant form of the electrostatic/virtual photon force from a charge is known, the derivation of a magnetic field when the charge moves was described as long ago as 1912, in an article by Page (*39*), who sought to bolster Einstein's hotly contested theory of special relativity. In short, a magnetic field is simply a tiny relativistic change in the powerful electrostatic field and, when a charge accelerates, that change is manifest on other charges nearby. Thus a changing current can induce an EMF in a nearby conductor. There is a certain irony to the fact that one of the best relativistic expositions of Faraday induction, starting from Eqs. [31] and [32], is given in Purcell's excellent undergraduate text on electromagnetism (*36*) and, as an exercise, the author has used that text as a starting point to calculate from Eq. [31] the mutual induction between two rings of conductor and thence the EMF induced by a rotating magnetic moment. (That calculation will not be reproduced here as it is too remote from NMR.)

Standing back from the experiment, the electromotive force around the Hertzian loop can be viewed as a torque, and such a view is consistent with the idea that the Lorentz transformation needed to calculate an induced EMF from Eqs. [31] and [32] can be viewed as a rotation. Quantum electrodynamically, virtual photons have four polarization states, in contrast to the two found in real photons, and the extra states are related to the classical vector magnetic and scalar potentials. Correspondingly, they carry angular momentum in their spin and orbital terms and are therefore capable of exerting a torque on the electrons in the receiving coil and a reaction on the nuclei. The interested reader may wish to peruse Feynman's popular exposition of QED (*29*) or more mathematical treatises such as the books by Jauch and Rohrlich (*31*) and Bjorken and Drell (*32, 33*) and Feyman's classic paper (*34*).

Considering the emission of virtual photons from the NMR sample now, Dicke's concept of coherence is still of vital importance as it determines the total amount of transverse or angular momentum carried. However, it is virtual photons that must be employed and it is coherent *virtual* emission, if we may coin such a term, that must be calculated. The fact that virtual photons carry no energy enables us to take liberties that are unthinkable when adopting a Hamiltonian viewpoint that is rooted in considerations of energy. For example, under Hamiltonian mechanics, one does not normally consider interac-

tions with a single nucleus because the act of interrogation of that nucleus changes its state. However, with virtual photons, it is perfectly legitimate to consider, for example, the expectation value of the EMF induced in an open-circuit receiving coil by a single nucleus, as was done earlier. This is possible because there is no exchange of energy—we are not actually performing a measurement. Once we close the circuit by putting resistance across its terminals, for example a voltmeter to perform a measurement, we perturb the system, and virtual photons possessing some energy can pass from the nuclei to the electrons in the receiving loop. From time to time, nuclear transitions will occur, the Uncertainty Principle granting this whole process a slackness that we are perhaps not used to dealing with. Thus in Dirac's quantum formulation of a free charged particle such as a proton, the latter is constantly jittering (*zitterbewegung* (*32*)) because of the random emission of virtual photons with a range of energies, positive and negative. Summarizing, in Feynman's words (*34*), "The Hamiltonian method is not well adapted to represent the direct action at a distance between charges because that action is delayed."

We are conscious that, against Heisenberg's advice, we are placing heavy emphasis on a classical concept that cannot actually be measured—the voltage induced in an open-loop circuit. However, that concept is so deeply embedded in our understanding of classical electrodynamics and makes so much intuitive sense that we cannot sidestep its implications—we *need* a quantum explanation for it. As unsatisfactory as virtual photons may be (try explaining electrostatic attraction!), they do at least give some insight at the quantum level into near-field interactions, rather than simply performing the energy balancing act of earlier work. They represent the best efforts of modern field theory.

Returning to the real world, two general comments are in order. First, no circuit is ever completely open as there is always capacitance present, and there is a link between the perturbing influence of that capacitance in our Hertzian loop and the extent of emission of energy (real photons); as a consequence, the higher the frequency, the more important both become. However, while capacitance can allow current to flow, the reaction B_1 field created in the rotating frame is then parallel to the precessing nuclear spins and so causes no nutation and no change of energy. It is thus a perturbation that does not affect the analysis significantly unless the coil is close to self-resonance and its own resistance can dissipate significant energy as heat, and we have consciously avoided that situation. Only a *resistance* across the coil terminals—the one energy-dissipative mechanism known to electronics—can cause current to flow in the correct phase so as to create a reaction B_1 field that nutates magnetization toward the z axis. Conservation of energy demands no less.

Second, with regard to spin noise, there is a facet of the experiment that seems to have escaped attention. From an experimental measurement system in thermal equilibrium, we appear to be getting information—the spectrum of the water—at no cost! We have taken great pains to ensure that any noise currents from the preamplifier that could drive the NMR system are negligible (a very low noise figure) and yet the information is there. Presumably, the preamplifier's electrons must effectively be cold at its field effect transistor's internal junction, giving the term "noise-temperature" for a preamplifier a rather more concrete meaning.

In conclusion, we have shown that both the FID and the spin noise can be accurately predicted by near-field classical theories that have nothing to do with the emission of radiation. Thus popular expositions of magnetic resonance that describe the phenomenon as the absorption and emission of radio waves are wrong. The theory of coherent spontaneous emission must be replaced by one of coherent emission of virtual photons, while spin noise may be considered a consequence of the random emission of virtual photons. The venerable classical concept of Faraday induction remains the easiest route to comprehension and calculation of voltages associated with magnetic resonance phenomena at those B_0 magnetic field values currently in use. Only when the size of the sample approaches the wavelength of any radiation need voltages associated with the latter be taken into account. This is beginning to be the case in certain high-field human imaging experiments and an example of the modifications required to the mathematics is given in Ref. (*40*).

POSTSCRIPT—EXPERIMENTAL DETAILS

The experiments now to be described in detail relied heavily for efficacy and accuracy on careful radiofrequency electronic fabrication. All results were obtained in an 80-cm horizontal bore, 1.5-T imaging magnet manufactured by Magnex Ltd. (Abingdon, UK), working with protons in water at a frequency of 63.877 MHz. The spectrometer was made by Surrey Magnetic Imaging Systems (SMIS, Guildford, UK). All impedance and gain measurements, unless otherwise specified, were made with a new Hewlett–Packard 8712 ET network analyzer.

FID Measurements

A diagram of the probe used is shown in Fig. 1. Both transmitting and receiving coils were single-gap, Hertzian loops. Experiments were executed inside a closed cylindrical shield of length 768 mm and diameter 540 mm to prevent the intrusion of exterior interference. The dominant resonant mode of the cavity created by the shielding was at 426 MHz, well above the frequency of interest. During transmission, power was applied through a crossed-diode switchbox (Fig. 9) to the outer, tuned and matched transmission loop. The latter was in the xz plane, was made of 8-mm-diameter copper tubing, and was of nominal radius 62.5 mm. Note that the matching was via a half-wavelength balun with symmetrical fixed tuning and matching capacitors C_t and C_m, respectively, and a small, fine-tuning capacitor C_{tf} (*19*). The aim of this construction was

to minimize electrostatic coupling between transmitting and receiving coils, and the isolation during transmission, as measured with the network analyzer, was −60.3 dB. During signal reception when the transmitter was off, the crossed-diode switchbox placed a high impedance in the transmitter feedline, for the self-capacitance of the diodes was cancelled with the aid of the tuned circuit comprising L_3 and C_3. The length of the line between the box and the transmitting loop was adjusted (slightly greater than λ/4) so that, thanks to its high-impedance termination, it acted as an inductor and resonated with the matching capacitor C_m. This created a parallel tuned circuit which impeded the flow of current around the transmitter coil, increasing the isolation by an extra 21.2 dB. Thus the transmitter loop was considered a negligible perturbation to the system during signal reception and could be ignored.

The untuned receiving coil, made of copper tube of diameter 8.0 mm, was also a circular Hertzian loop, as this type of coil lends itself well to analytical calculations. It was placed in the *yz* plane orthogonal to the transmitting loop, with a 5-mm gap and an inner circumference of 290.0 ± 0.3 mm. Thus its average radius was 50.15 mm and its calculated reactance (*23*), with high-frequency correction, was 67 Ω. For verification and setup purposes only, the loop was temporarily tuned to 67.877 MHz with a capacitor across the gap. Thus the calculated reactance was verified to within ±2 Ω by measuring the capacitance. (Stray capacitance and uncertainty as to the exact distribution of current on the surface of a loop render the comparison a little inaccurate.) Tuning of the loop to the desired frequency was with the aid of two symmetrically placed, weakly coupled (<−40 dB), small, orthogonal pickup coils (not shown) and the network analyzer in transmission mode (*19*). One pickup coil acted as a transmitter coupled by mutual induction and the other as a receiver coupled likewise. Having verified the loop reactance, the tuned loop and pickup coils were pressed into further service. Resistances in value between 200 and 2000 Ω with minimal lead length were placed directly across the loop gap. A calibration plot was then made of the transfer function of the assembly in decibels versus load resistance in ohms at 63.877 MHz. In this manner, the resistance of any arbitrary load placed across the gap could be determined from the calibration curve, which was fitted accurately both to the theoretical curve and somewhat more simply to a third-order polynomial. Note that a network analyzer is unreliable for high-impedance measurements.

Our aim now was to connect two low-loss, nominally 50-Ω coaxial cables (Belden type 9311) across the gap in the receiving loop without compromising the isolation between transmitting and receiving coils. One cable was to allow the remote connection of resistances across the gap, thereby allowing the loading on the loop to be varied. (Direct connection of resistances, as in the calibration experiment above, destroys B_0 homogeneity as the leads on resistors are ferromagnetic.) The other cable was to connect to the preamplifier. The method of connection was to take a cable, bared of outer insulation, inside a supporting copper tube connected half way around the Hertzian loop and thence *inside* one side of the loop up to the gap, as shown in Fig. 1. The base of the support was connected to the shield. This strategy preserved the balanced nature of the receiving assembly (*41*) and ensured that its measured characteristics, such as effective inductance, did not vary with vagaries such as transmitter cable routing. The first cable was connected and its length, originally a little longer than λ/2, was cut back until the resonant frequency of the still-tuned loop returned to the Larmor frequency. The cable was found to be 1.79 m in length and to have a velocity factor of 0.762. The cable was now loaded with resistances R_v of values between 200 and 2000 Ω at its open, remote end and their loading of the tuned circuit was determined from the amplitude of the transfer function, via the calibration curve. It was found that the loading across the gap could be accurately represented by the chosen resistance value in parallel with $R_c = 2380 \pm 30$ Ω. The value R_c represented the loss in the λ/2 cable. Note that use of *Q*-factor measurements in this situation to obtain loading will give erroneous results, as the line is essentially a second tuned circuit in parallel with that of the loop.

The second cable, a quarter wavelength long, was now also connected to the loop in the same manner, and the λ/2 cable was temporarily disconnected. The new cable led to the tuned preamplifier of Fig. 10a that had a noise figure of 0.45 dB and a measured input impedance from the network analyzer of the order of 5 Ω resistive. Its design is unremarkable and will not be discussed further. The preamplifier's input variable capacitor C_4 was now minutely adjusted to bring the loop resonance back to the Larmor frequency and thus to provide resistive loading across the gap. In the process, the noise figure was degraded to 0.55 dB. From the transfer function calibration, the loading was measured as 534 ± 5 Ω, in rough accord with the 5-Ω input resistance and the transformation properties of a λ/4 cable. The λ/2 cable was now reconnected and the loop's tuning capacitor removed. Thus the loading across the loop gap could be considered to comprise whatever resistance value R_v was placed across the end of the λ/2 cable in parallel with 2380 Ω from the cable loss and 534 Ω from the preamplifier, as shown in Fig. 2. Any stray capacitance across the loop gap was assumed to be subsumed in the high-frequency correction for the inductance value.

The output of the preamplifier was connected either to the spectrometer during "setup" or to a triggered Tektronix type 2465ADM oscilloscope (with the 50-Ω input impedance option selected) during signal reception. The gain of the preamplifier, plus losses in its λ/4 cable and the long output cable leading away from the magnetic field to the oscilloscope, was 16.4 ± 0.2 (29.5 ± 0.1 dB) as measured with the network analyzer, once the high input impedance of the preamplifier and the source impedance at the cable end (52.2 Ω) had been taken into account. The calibration of the oscilloscope was compared to that of the new network analyzer, and the oscilloscope's readings were found to need multiplication by 1.02 ± 0.005. To

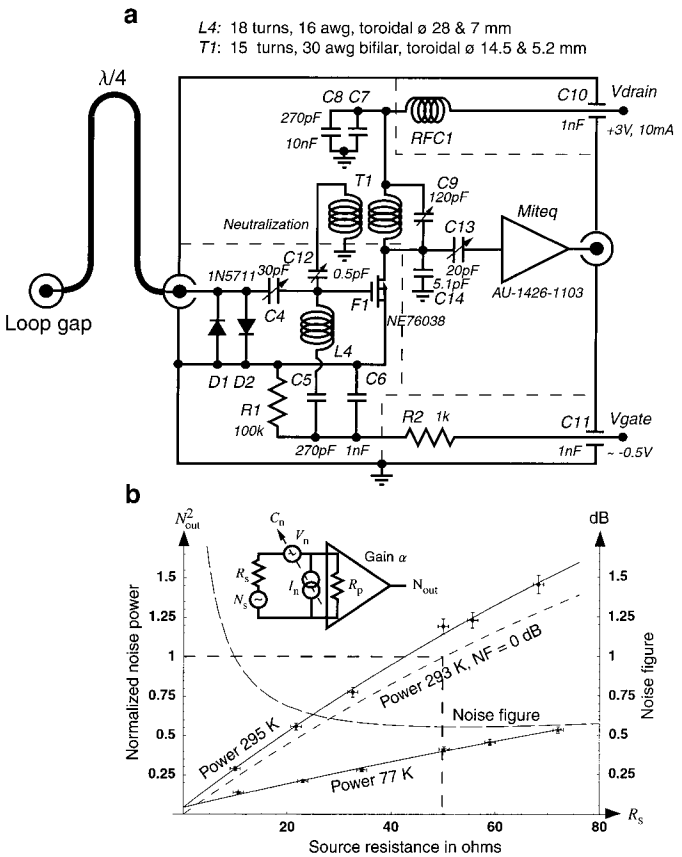

FIG. 10. (a) The preamplifier and its connection to the receiving loop or coil. C_4 and L_4 are resonant and the input impedance is therefore low and resistive ($\sim$5 Ω). Neutralization is provided by drain signal inversion in transformer T_1 and capacitor C_{12}. For the spin noise experiment, the crossed diodes were replaced by a PIN diode to give better protection from the transmitter pulses during "setup." (b) Characterization of the preamplifier (λ/4 line included) with a standard noise model. Normalized noise output power and noise figure in decibels are plotted as a function of source resistance. In the model, R_p is the (noiseless) amplifier input resistance (534 Ω) and R_s is the source resistance with root mean square noise voltage $N_s = (4kTR_s)^{1/2}/\sqrt{\text{Hz}}$. V_n and I_n are the amplifier voltage and current noise sources, respectively, with correlation coefficient C_n. The noise output power is normalized to that pertaining to a 50-Ω source at 293 K with a noiseless preamplifier. Experimental points are given for T = 77 and 295 K and the solid lines are least-squares fits obtained with $V_n = 0.17 \pm 0.05$ nV/$\sqrt{\text{Hz}}$, $I_n = V_n/50 = 3.24$ pA/$\sqrt{\text{Hz}}$, and $C_n = 1\ +0/-0.5$. The noise figure at 50 Ω was 0.55 ± 0.1 dB. The power plots are curved because the input impedance of the preamplifier is not infinite.

summarize, the untuned receiving loop was effectively connected to a high-gain, calibrated oscilloscope whose effective input impedance at the Larmor frequency could be any desired value up to $436 \pm 4\ \Omega$ with a preamplification factor of 16.1 ± 0.2 allowing for the gain correction. The equivalent circuit is shown in Fig. 2.

The sample was a sphere of water in a ping-pong ball placed at the center of the two loops. The sample's weight was 26.24 ± 0.01 g and it was doped with a little nickel chloride to reduce its relaxation times to the order of 100 ms. A 50-μs 90° pulse was applied to the sample with the aid of the transmitting loop and the initial amplitude of the resulting free induction decay at the output of the preamplifier was measured with the aid of the oscilloscope to an estimated accuracy of ± 0.5 mV. It was ascertained that the preamplifier was unsaturated and was giving its full gain. The experiment was then repeated for various values of loading resistance R_v placed at the end of the λ/2 cable.

Spin Noise Measurements

Prior to undertaking any experiments, it was ensured that the preamplifier's noise behavior (λ/4 line included) was thoroughly understood by characterization with the standard model (*24*) shown in Fig. 10b. R_p is the preamplifier input resistance (534 Ω as before) and R_s is the source resistance with root mean square noise voltage $N_s = (4kTR_s)^{1/2}/\sqrt{\text{Hz}}$, experimental points being given for 77 and 295 K. V_n and I_n are the amplifier voltage and current noise sources, respectively, with correlation coefficient C_n. The solid lines are least-squares fits to the experimental data. The noise output power is normalized to that for a 50-Ω source at 293 K (symmetrically broken line) and a preamplifier of noise figure zero. The best fit was obtained with $V_n = 0.17 \pm 0.05$ nV/$\sqrt{\text{Hz}}$, $I_n = V_n/50 = 3.24$ pA/$\sqrt{\text{Hz}}$, and $C_n = 1\ +0/-0.5$. The minimum noise figure (asymmetrically broken line) was 0.55 ± 0.1 dB.

Annealed, copper-clad aluminum wire of nominal diameter 50 μm was purchased from California Fine Wire (Grover City, CA). However, the diameter was found to vary greatly and a section of only 37-μm diameter was actually used. The copper comprised 12% by volume and thus the nominal radius of the aluminum was 0.938 that of the wire. The wire was plated with diamagnetic copper (volume susceptibility -9.631×10^{-6}) to a final diameter of 61 μm to annul the paramagnetic susceptibility of the aluminum (20.764×10^{-6}) using the Udylite UBAC Interplate bright acid copper process (Enthone-OMI, Concord, Ontario, Canada) and $CuSO_4$–$5H_2O$ at 180 g/L, H_2SO_4 at 53 g/L, and HCl at 80 mg/L. Plating current was 20.2 mA for 24 min 45 s. The washed and dried wire was then spaced with silk thread and 20.5 turns were carefully wound onto a 5-mm precision NMR tube (Norell, Inc., Landisville, NJ) by gloved hand where it was lightly glued in place with cyanomethacrylate. The silk was later removed. The winding spanned 6 mm, rather than the 5 mm needed theoretically for maximum NMR resistance, as this length cancelled any second-order field perturbation due to residual wire susceptibility. The tube was then filled with degassed water, capped, and laid in a cradle, as shown in Fig. 4. Its leads were brought to a printed circuit board ground plane 40 mm away—a relatively large separation designed to minimize B_0 inhomogeneity caused by the susceptibility of the printed circuit board and its components. One lead was attached to a 1–3 pF variable *series* capacitor to ground, as shown. Effective stray capacitance was estimated to be roughly 2 pF. The capacitance was added

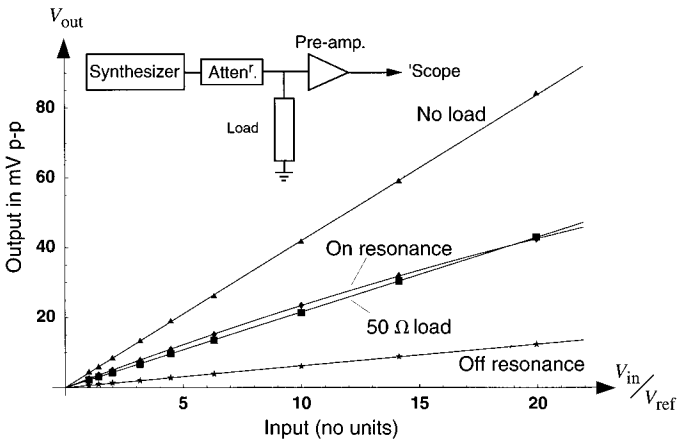

FIG. 11. A continuous wave experiment to verify the NMR and coil resistances. The preamplifier output is plotted against frequency synthesizer input for four load conditions: no load (open circuit); 50-Ω load, NMR coil and sample off resonance by 1 kHz, NMR coil and sample on resonance. For the latter case, note the curvature in the plot caused by the onset of saturation as the input voltage is increased. It is fitted by a second-order Taylor expansion. The desired resistances are calculated from the slopes at the origin of the lines/curve.

reluctantly to cancel the reactance of the coil ($\sim j550\ \Omega$), as mentioned earlier. The other lead was attached to the λ/4 cable leading to the preamplifier and also to the λ/2 cable which now enabled transmitter power to be applied for the purpose of shimming on the FID. However, a PIN diode, rather than a crossed-diode, switching system was now used to protect the preamplifier from the pulses and possible noise from the transmitter. As the loading on the coil was, as before, 436 Ω, the effective Q-factor of the assembly was roughly unity. The cables also allowed power to be passed from the transmission port of the network analyzer to the λ/4 cable and then to the reception port. The reactance of the coil was considered cancelled by the reactance of the capacitor when the transfer function at 63.877 MHz was a minimum. A dip of −12.8 dB was observed on the bench, implying that the resistance of the coil was about 8 Ω. (N.B. the coil was not designed for optimum signal-to-noise ratio, but for high NMR resistance.) The cables passed through brass compression fittings on a copper end-flange (not shown). The top of the cradle was put in place and secured, and the assembly was mounted in the shim set which had its own RF shield to which the copper end-flange was attached. No leakage of interference could be detected.

NMR resistance was directly measured by a continuous wave experiment. A frequency synthesiser was attached to the λ/2 cable and the output of the preamplifier was observed with an oscilloscope on and off resonance (1 kHz) for various input voltages. For calibration purposes, the output was also plotted with a 50-Ω load in place of the coil and its capacitor and with no load. The results are shown in Fig. 11, and from the slope of the off-resonance plot line, the resistance of the coil is 8.2 ± 0.2 Ω, in good agreement with the network analyzer and noise measurements. The on-resonance plot was fitted to second order to allow for the onset of saturation at higher powers and from the gradient at the origin, the coil plus NMR resistance is 73 ± 4 Ω. Thus the NMR resistance is 65 ± 4 Ω.

Noise was measured with the aid of the spectrometer and its software and once the instrument's parameters had been set, they remained the same for all measurements. To calibrate the system, identical cables to those seen in Fig. 4 were made and the noises from a set of resistors at 293 and 77 K on the end of the λ/4 cable were measured. The λ/2 cable and PIN diode switch, with the transmitter connected but gated off, were found to increase the noise figure slightly to 0.7 dB. In the absence of a field-frequency lock, random changes of B_0 field were a nuisance when attempting to measure spin noise. These were tracked down to the motion of the large garage door in the underground parking lot that is part of our building. Once this problem had been circumvented with late nights, spectra could be reliably obtained. The sum of the amplitude (as opposed to power) transforms had no spectral detail. Further, taking the Fourier transforms of the *differences* between pairs of noise data and using these 32 arrays to create a new power spectrum did not change the spectral width or height; only the signal-to-noise ratio was diminished by $\sqrt{2}$.

ACKNOWLEDGMENTS

We acknowledge numerous colleagues who have debated the contents of this paper over several years. In particular, B. Bhakar, N. Davidson, H. Evitar, H. M. Georgi, J. S. Hyde, R. Somorjai, and W. S. Warren have been very helpful. E. L. Hahn has supplied much useful criticism and we are particularly grateful to him for suggesting the challenge of explaining spin noise. We thank Glen Kolansky for invaluable help with the construction of the probes and preamplifier. Finally, we thank J. Wright for alerting us to the existence of Ref. (*12*).

Note added in proof. With regard to Fig. 8 and spin noise, a recently published paper is of import. It is M. P. Augustine, S. D. Bush, and E. L. Hahn, Noise triggering of radiation damping from the inverted state, *Chem. Phys. Lett.* **322,** 111–118 (2000).

REFERENCES

1. W. Heitler, "The Quantum Theory of Radiation," Clarendon Press, Oxford, 1936.
2. J. D. Macomber, How does a crossed-coil NMR spectrometer work? *Spectrosc. Lett.* **1,** 131–137 (1968).
3. N. Bloembergen and R. V. Pound, Radiation damping in magnetic resonance experiments, *Phys. Rev.* **95,** 8–12 (1954).
4. A. Abragam, "The Principles of Nuclear Magnetism," Clarendon Press, Oxford, 1961.
5. R. H. Dicke, Coherence in spontaneous radiation processes, *Phys. Rev.* **93,** 99–110 (1954).
6. E. M. Purcell, Nuclear magnetism in relation to problems of the liquid and solid states, *Science* **107,** 433–440 (1948).
7. E. L. Hahn, Nuclear induction due to free Larmor precession, *Phys. Rev.* **77,** 297–298 (1950).
8. E. L. Hahn, Spin echoes, *Phys. Rev.* **80,** 580–594 (1950).
9. K. W. H. Stevens, The Hamiltonian formalism of damping in a tuned

circuit, *Proc. Phys. Soc.* **77,** 515–525 (1961), and references therein.

10. J. Rosenthal, Comments on "How does a crossed-coil NMR spectrometer work?" *Spectrosc. Lett.* **1,** 255–257 (1968).

11. J. D. Macomber, Reply to "Comments on 'How does a crossed-coil NMR spectrometer work?'" *Spectrosc. Lett.* **1,** 265–270 (1968).

12. R. H. Dicke, Discussion on: How does a crossed-coil NMR spectrometer work? *Spectrosc. Lett.* **1,** 415–419 (1968).

13. T. Sleator and E. L. Hahn, Nuclear spin-noise, *Phys. Rev. Lett.* **55,** 1742–1745 (1985).

14. T. Sleator, E. L. Hahn, C. Hilbert, and J. Clarke, Nuclear spin-noise and spontaneous emission, *Phys. Rev. B* **36,** 1969–1980 (1987).

15. F. Bloch, Nuclear induction, *Phys. Rev.* **70,** 460–474 (1946).

16. M. Guéron and J. L. Leroy, NMR of water protons. The detection of their nuclear spin noise, and a simple determination of absolute probe sensitivity based on radiation damping, *J. Magn. Reson.* **85,** 209–215 (1989).

17. M. A. McCoy and R. R. Ernst, Nuclear spin noise at room temperature, *Chem. Phys. Lett.* **159,** 587–593 (1989).

18. H. C. Ohanian, "Classical Electrodynamics," Allyn and Bacon, Boston, 1988.

19. C.-N. Chen and D. I. Hoult, "Biomedical Magnetic Resonance Technology," Hilger, Bristol, 1989.

20. C. W. Helstrom, "Probability and Stochastic Processes for Engineers," 2nd ed., Maxwell–Macmillan, New York, 1991.

21. W. R. Smythe, "Static and Dynamic Electricity," 3rd ed., McGraw–Hill, New York, 1968.

22. D. I. Hoult, The NMR receiver: A description and analysis of design, *Prog. NMR Spectrosc.* **12,** 41–77 (1978).

23. F. E. Terman, "Radio Engineers' Handbook," McGraw–Hill, New York, 1943.

24. C. D. Motchenbacher and J. A. Connelly, "Low-Noise Electronic System Design," Wiley, New York, 1993.

25. E. E. Zepler and S. W. Punnett, "Electronic Devices and Networks," Blackie, London, 1963.

26. D. I. Hoult and B. Bhakar, NMR signal reception: Virtual photons and coherent spontaneous emission, *Concepts Magn. Reson.* **9,** 277–297 (1997).

27. D. I. Hoult, Fast recovery with a conventional probe, *J. Magn. Reson.* **57,** 394–403 (1984).

28. P. B. Roemer, W. A. Edelstein, C. E. Hayes, S. P. Souza, and O. M. Mueller, The NMR phased array, *Magn. Reson. Med.* **16,** 192–225 (1990).

29. R. P. Feynman, "QED," Princeton Univ. Press, Princeton, NJ, 1985.

30. P. Davies (Ed.) "The New Physics," Cambridge Univ. Press, Cambridge, 1989.

31. J. M. Jauch and F. Rohrlich, "The Theory of Photons and Electrons," 2nd ed., Springer-Verlag, New York, 1976.

32. J. D. Bjorken and S. D. Drell, "Relativistic Quantum Mechanics," McGraw–Hill, New York, 1964.

33. J. D. Bjorken and S. D. Drell, "Relativistic Quantum Fields," McGraw–Hill, New York, 1965.

34. R. P. Feynman, Space–time approach to quantum electrodynamics, *Phys. Rev.* **76,** 769–789 (1949).

35. J. D. Jackson, "Classical Electrodynamics," 2nd ed., Wiley, New York, 1975.

36. E. M. Purcell, "Electricity and Magnetism," 2nd ed., McGraw–Hill, New York, 1985.

37. E. F. Taylor and J. A. Wheeler, "Spacetime Physics," Freeman, San Francisco, 1966.

38. G. G. Ross, "Grand Unified Theories," Benjamin/Cummings, Reading, MA, 1984.

39. L. Page, A derivation of the fundamental relations of electrodynamics from those of electrostatics, *Am. J. Sci.* **34,** 57–68 (1912).

40. D. I. Hoult, Sensitivity and power deposition in a high-field imaging experiment, *J. Magn. Reson. Imaging* **12,** 46–67 (2000).

41. R. E. Burgess, The screened loop aerial, *Wireless Eng.* **October,** 492–499 (1939).